

Articles

Linear and Hyperbranched Glycopolymer-Functionalized Carbon Nanotubes: Synthesis, Kinetics, and Characterization

Chao Gao,^{*,†,‡} Sharmila Muthukrishnan,[‡] Wenwen Li,[†] Jiayin Yuan,[‡] Youyong Xu,[‡] and Axel H. E. Müller^{*,‡}

College of Chemistry and Chemical Engineering, Shanghai Jiao Tong University, 800 Dongchuan Road, Shanghai 200240, P. R. China, and Macromolecular Chemistry II, Bayreuth University, D-95440 Bayreuth, Germany

Received September 26, 2006; Revised Manuscript Received January 19, 2007

ABSTRACT: Linear and hyperbranched glycopolymers, a kind of sugar-containing polymers, were grown successfully from surfaces of multiwalled carbon nanotubes (MWNTs) by the “grafting from” strategy with good controllability and high reproducibility. Linear glycopolymer was grafted from the surfaces of MWNTs by surface-initiated atom transfer radical polymerization (ATRP) of 3-*O*-methacryloyl-1,2:5,6-di-*O*-isopropylidene- α -D-glucopyranose (MAIG) with Cu^IBr/HMTETA (1,1,4,7,10,10-hexamethyltriethylenetetramine) at 60 °C in ethyl acetate. After hydrolysis of polyMAIG in 80 wt % formic acid for 48 h, water-soluble poly(3-*O*-methacryloyl- α , β -D-glucopyranose) (polyMAG)-grafted MWNTs were obtained. The kinetics were investigated by carrying out the polymerizations using 2-bromo-2-methylpropionyl-immobilized MWNTs (MWNT-Br) as the macroinitiator in the absence or presence of ethyl 2-bromoisobutyrate as sacrificial initiator. In both cases a linear dependence of molecular weight on conversion was obtained, and the polymer amounts grafted on MWNTs could be well controlled in a wide range by the reaction time and monomer conversion. Coupling was found in the GPC curves of free polymer when the conversion of monomer reached ca. 45–50%. This clearly indicates that coupling reactions are more predominant than the conventional ATRP in a homogeneous solution without CNTs, where no coupling occurred despite of very high conversion of this monomer (>80%). Hyperbranched glycopolymers (HPGs) were also grafted from the surfaces of MWNTs by self-condensing vinyl copolymerization (SCVCP) of the monomer, MAIG, and inimer, 2-(2-bromoisobutyryloxy)ethyl methacrylate (BIEMA, AB*) via ATRP with bis(triphenylphosphine)nickel(II) bromide ((PPh₃)₂NiBr₂) at 100 °C in ethyl acetate. After deprotection in formic acid, hyperbranched glycopolymers with high density of hydroxyl groups functionalized MWNTs were achieved. The novel water-soluble biocompatible glycopolymer-grafted CNTs have fascinating potentials in the fields of tissue engineering and bionanomaterials.

Introduction

Carbon nanotubes (CNTs)¹ are one of the most fascinating nanoobjects, which have a wide range of applications. To explore and realize their potentials, the functionalization of CNTs has been investigated to make soluble individual carbon nanowires available.^{2,3} In this regard, grafting polymers onto or from the convex surfaces of CNTs to prepare polymer-coated nanotubes is of intriguing interest to both scientists and engineers.⁴ Many techniques including esterification,⁵ “click” chemistry,⁶ layer-by-layer self-assembly,^{7,8} pyrene moiety adsorption,⁹ radical coupling,¹⁰ anionic coupling,¹¹ radical polymerization,¹² supercritical CO₂-solubilized polymerization or coating,¹³ γ -ray irradiation,¹⁴ cathodic electrochemical grafting,¹⁵ polycondensation,¹⁶ reversible addition fragmentation chain-transfer (RAFT) polymerization,^{17–19} anionic polymerization,²⁰ ring-opening polymerization,^{21,22} and atom transfer radical polymerization (ATRP)^{23–26} have been employed to functionalize CNTs.

Among them, the ATRP approach is quite efficient and versatile. Up to now, different kinds of ATRP-active monomers, e.g., (meth)acrylates,^{7,23–28} styrenics,^{7,29} and acrylamides,^{30,31} have been polymerized and also block copolymers have been grafted from the surfaces of CNTs.^{23,32} It has been shown that the grafting efficiency can be controlled to some extent by the feed ratio of monomer to CNT-based macroinitiator.^{23,27–30} The polydispersity index (PDI) of free polymer in the presence of sacrificial initiator is normally broader than those without CNTs.²⁸ Therefore, investigation of the polymerization kinetics is fundamentally required to understand the reaction process and reveal the reasons of the broader PDI. However, a kinetic study using ATRP in the presence of multiwalled carbon nanotubes (MWNTs) has never been reported before. In the cases of single-walled carbon nanotubes (SWNTs), incompatible conclusions were obtained: controllable²⁴ or noncontrollable polymerization.²⁵

In order to improve the solubility or dispersibility of CNTs in water, and then to apply them in aqueous solution, grafting water-soluble polymers onto CNTs are of great interest. Via the “grafting to” approach, poly(sodium 4-styrenesulfonate),³³ poly(*m*-aminobenzenesulfonic acid) (PABS),³⁴ poly(2-vinylpy-

* Corresponding authors. E-mail: chaogao@sjtu.edu.cn (C.G.); axel.mueller@uni-bayreuth.de (A.H.E.M.).

[†] Shanghai Jiao Tong University.

[‡] Bayreuth University.

ridine),³⁵ poly(propionylethylenimine-co-ethylenimine (PPEI-EI),³⁶ oligomeric and polymeric species containing poly(ethylene glycol) (PEG) blocks, and poly(vinyl alcohol) (PVA) and its related copolymer poly(vinyl acetate-co-vinyl alcohol) (PVA-VA),⁵ as well as poly(amido amine) (PAMAM) dendrimers³⁷ have been successfully tethered to surfaces of CNTs. Via the “grafting from” or in situ polymerization approach, anionic polymers such as poly(acrylic acid),^{7,38} poly(sodium 4-styrenesulfonate)⁷ and sulfonated polyaniline,³⁹ cationic polymers such as poly(2-dimethylaminoethyl methacrylate) (PDMAEMA)^{27,40} and poly(2-diethylaminoethyl methacrylate) (PDEAEDA),⁴¹ and nonionic polymers such as poly(glycerol monomethacrylate) (PGMA),²⁸ poly(*N*-isopropylacrylamide) (PNIPAAm),^{18,30,31} and poly(*N*-(2-hydroxypropyl)methacrylamide) (PHPMA)¹⁹ have been grown from CNTs. The water-soluble polymer-functionalized CNTs can be used to prepare temperature-responsive nanodevices,³⁰ self-assembly multilayer nanocylinders or films,⁷ magnetic nanowires,⁴¹ and metal nanocrystals^{28,42} or quantum dots (QDs)/CNT nanohybrids.⁴⁰ Now, the relevant works are in the ascendant, promising applications of these materials.

Besides linear polymers, hyperbranched polymers⁴³ with highly branched three-dimensional architecture were also tried to functionalize CNTs because of their multifunctional groups, high solubility, and other unique properties. Via in situ ring-opening polymerization, multihydroxy hyperbranched poly(3-ethyl-3-hydroxymethyloxetane) was grafted from surfaces of MWNTs with degrees of branching (DB) of 0.25–0.42, and polymer contents of 20–87 wt % were obtained.⁴⁴ By use of the in situ polycondensation or “grafting to” approach, multi-amino hyperbranched PAMAM was also coated onto MWNTs with polymer contents of 30–70 wt %.⁴⁵ Recently, Hong et al. grafted hyperbranched polymer from surfaces of MWNTs by self-condensing vinyl polymerization (SCVP) of the 2-((bromobutyl)oxy)ethyl acrylate (BBEA) inimer with a high polymer content (80 wt %).⁴⁶ The multifunctional hyperbranched polymer-functionalized CNTs offer a versatile platform for tailoring and fabricating novel hybrid nanomaterials and nanodevices.

On the other hand, to graft biocompatible polymers onto CNTs is arousing more and more interest, due to the great significance of the resulting polymer–CNT nanohybrids in the fields of bionanotechnology. Poly(ϵ -caprolactone) (PCL) was successfully grafted from CNTs by ring-opening polymerization.²¹ It was reported that PCL grafted covalently on CNTs has the same biodegradability as the free PCL without CNTs, and it can be enzymatically degraded within 4 days in a phosphate buffer solution in the presence of pseudomonas lipase, whereas the carbon nanotubes still retain their tubelike morphology.²¹ Poly(L-lactic acid) (PLLA) with different molecular weights were coated onto MWNTs by the “grafting to” approach.⁴⁷ Through noncovalent complexation of the nanotubes with a water-soluble, biocompatible polymer chitosan at room temperature, diameter-selective dispersion of SWNTs was accomplished.⁴⁸ Sun et al. demonstrated that galactose derivatives-functionalized CNTs were effective in the capturing of pathogenic *Escherichia coli* in solution.⁴⁹ In addition, phospholipid, poly-L-lysine, proteins, and DNA were also immobilized or adsorbed onto CNTs, especially SWNTs.⁵⁰

In this article, we report the grafting of biocompatible, water-soluble, and linear and hyperbranched glycopolymers from surfaces of MWNTs by ATRP⁵¹ of 3-*O*-methacryloyl-1,2:5,6-di-*O*-isopropylidene-D-glucofuranose (MAIG) and self-condensing vinyl copolymerization (SCVCP) of MAIG and AB* inimer,

2-(2-bromoisobutyryloxy)ethyl methacrylate (BIEM). The polymerization kinetics is investigated in detail. The resulting multihydroxy glycopolymer-functionalized CNTs have potential applications in the fields of tissue engineering and bionanotechnology. The results of kinetics enable us to understand the surface-initiated ATRP more deeply and to achieve results with better controllability.

Experimental Section

Materials. The multiwalled carbon nanotubes (MWNTs) made from the chemical vapor deposition method were purchased from Tsinghua-Nafine NanoPowder Commercialization Engineering Centre in Beijing (>95% purity). MWNT-based macroinitiator, 2-bromo-2-methylpropionyl-immobilized MWNTs (MWNT–Br), was synthesized according to previous procedures.²³ The density of initiating group of MWNT–Br, calculated from corresponding TGA weight loss data and elemental analysis, is ca. 0.421 mmol per gram MWNT–Br, 0.526 mmol per gram of neat MWNTs, or ca. 6.3 initiating groups per 1000 carbons. The monomer, 3-*O*-methacryloyl-1,2:5,6-di-*O*-isopropylidene-D-glucofuranose (MAIG), was synthesized by the reaction of 1,2:5,6-di-*O*-isopropylidene-D-glucofuranose and methacrylic anhydride in pyridine and purified by vacuum distillation as reported by Klein et al.⁵² The methacrylic AB*-type inimer, 2-(2-bromoisobutyryloxy)ethyl methacrylate (BIEM), was synthesized by the reaction of 2-bromoisobutryl bromide with 2-hydroxyethyl methacrylate in the presence of pyridine and purified by high-vacuum distillation as reported previously.⁵³ Ethyl 2-bromoisobutyrate (98%, Aldrich), bis(triphenylphosphine)nickel(II) bromide ((PPh₃)₂NiBr₂, 99%, Aldrich), and 1,1,4,7,10,10-hexamethyltriethylenetetramine (HMTETA, 97%, Aldrich) were used as received. CuBr (98%, Aldrich) was purified by stirring overnight in acetic acid. After filtration, it was washed with ethanol and ether and then dried. Ethyl acetate was distilled and stored under nitrogen.

Characterization and Instrumentation. The apparent molecular weight and polydispersity index (PDI) of both linear and hyperbranched polymers were measured by gel permeation chromatography (GPC) using THF as eluent at a flow rate of 1.0 mL/min at room temperature. Column set: 5 μ m PSS SDV gel, 10², 10³, 10⁴, 10⁵ Å, 30 cm each. Detectors: Waters 410 differential refractometer and Waters photodiode array detector operated at 254 nm. Narrow polystyrene (PS) standards (PSS, Mainz) were used for the calibration. ¹H NMR spectra were recorded with a Bruker AC-250 spectrometer. FT–IR spectra were recorded on a Bruker Equinox 55 spectrometer. Thermogravimetric analyses (TGA) were conducted on a PE TGA-7 instrument at a heating rate of 10 °C min^{−1} under nitrogen.

The *scanning force microscopy* (SFM) images were taken with a Digital Instruments Dimension 3100 microscope operated in tapping mode (free amplitude of the cantilever \approx 30 nm, set point ratio \approx 0.98, tip radius \approx 20 nm). The SFM samples for measurements were prepared by drop-coating with tetrahydrofuran (THF) solution of product, onto freshly cleaved mica surface. Transmission electron microscopy (TEM) studies were performed on a LEO 922 OMEGA electron microscope operating at 200 kV. The TEM samples were prepared by dropping either THF or methanol (for the deprotected products) solution of product onto a lacey carbon TEM sample grid (Agar S166–4 lacey carbon 400 mesh Cu). Scanning electron microscopy (SEM) images were recorded using a LEO 1530 Gemini microscope, and the samples of solid powder were loaded on the carbon film substrate.

Grafting Linear Glycopolymer from MWNTs. All polymerizations were carried out in a round-bottom flask sealed with a plastic cap. A representative example for grafting linear glycopolymer from surfaces of MWNTs with MWNT–Br and sacrificial initiator, ethyl 2-bromoisobutyrate, as co-initiators is described as follows. MWNT–Br (100.0 mg, 0.0421 mmol Br), ethyl 2-bromoisobutyrate (4.7 mg, 0.0241 mmol), CuBr (9.4 mg, 0.0655 mmol), HMTETA (15 mg, 0.0651 mmol), anisole (1 mL), and ethyl acetate (4.5 mL) were placed in a 25 mL flask, which was then

Table 1. Kinetics Investigation and Results for the ATRP of MAIG in the Presence of MWNT-Br and Ethyl 2-Bromoisobutyrate^a

code	time/h	convn/% ^b	$M_{n,app}$ ^c	PDI ^c	$M_{n,theo}$ ^d	$f_{wt}/\%$ ^e	MW _{TGA} ^f	E_{ini} ^g
1	0.5	18.7	8700	1.27	7050	38	1165	0.165
2	1.1	26.4	11 200	1.26	9960	42.5	1405	0.141
3	1.5	30.4	12 600	1.25	11 470	46	1620	0.141
4	2.5	35.0	15 700	1.22	13 200	50	1900	0.144
5	3.5	39.6	17 800	1.21	14 940	53.5	2190	0.147
6	4.5	44.6	19 600	1.22	16 820	55.5	2370	0.141
7	5.5	49.6	20 700	1.25	18 710	58	2625	0.140
8	7.5	52.3	23 000	1.26	19 730	60	2850	0.144
9	10.5	58.8	26 600	1.28	22 180	61.5	3040	0.137
10	19	76.7	34 300	1.33	28 930	69	4230	0.146
11	25	83.9	35 800	1.42	31 650	70.5	4540	0.143
12	29	~85.0	37 400	1.45	~32 060	71	4650	~0.145

^a The mole ratio of monomer/MWNT-Br/sacrificial initiator/Cu^IBr/HMTETA is 115/0.64/0.36/1/1. ^b Monomer conversion determined from NMR spectrum. ^c The apparent number-average molecular weight (M_n) and polydispersity index (PDI) of soluble polymer measured by GPC. ^d The theoretical molecular weight calculated with the equation: $M_{n,theo} \approx 115 \times \text{convn} \% \times 328$; herein, 115 represents the degree of polymerization (DP) at the monomer conversion of 100%, and 328 is the molar mass of the MAIG monomer. ^e The mass fraction of polymer in the product of MWNTs-g-polyMAIG, determined from TGA. ^f The average molecular weight of polymer grafted on MWNTs, calculated from TGA data with the equation, $MW_{TGA} = f_{wt}/[(1 - f_{wt}) \times 0.526 \times 10^{-3}]$; herein, "0.526" denotes the density of initiating group on the MWNT-Br (mmol/g). ^g Initiating efficiency for the MWNT-Br macroinitiator, calculated from the ratio of $MW_{TGA}/M_{n,theo}$.

sealed with a plastic cap. The solution was degassed using dry nitrogen with stirring for approximately 30 min. A mixture of MAIG and ethyl acetate (4.5 g, 1/1 by mass, 7.62 mmol of monomer) which was degassed by nitrogen previously was injected into the flask using a syringe. The flask was immersed in an oil bath at 60 °C under stirring. After a certain time, a sample was taken using syringe. After oxidation on exposure to air, the sample was separated by centrifuging. The transparent green solution was used to measure the monomer conversion by NMR and molecular weight by GPC, respectively. The black solid was washed with THF several times and dried in vacuum, affording a sample of linear glycopolymer-grafted MWNTs. This solid sample was then further characterized by TGA, NMR, FTIR, SFM, TEM, or SEM. The selected results are summarized in Table 1.

Grafting Hyperbranched Glycopolymer from MWNTs. The similar protocol to the case of linear glycopolymer was employed to graft hyperbranched glycopolymer from surfaces of MWNTs. Typically (the molar ratio of monomer to inimer, $\gamma = 1$), BIEM (1.06 g, 3.81 mmol) and the mixture of MAIG and ethyl acetate (2.5 g, 1:1 by mass, 3.81 mmol of MAIG) were added to a round-bottom flask containing MWNT-Br (101.0 mg, ca. 0.0425 mmol Br), (PPh₃)₂NiBr₂ (52.0 mg, 0.07 mmol), anisole (0.6 mL, reference of NMR spectrum), and ethyl acetate (2 mL) under nitrogen. The flask was then sealed with a plastic cap and immersed in an oil bath at 100 °C under stirring. After a certain time, a sample was taken by using a syringe. After oxidation on exposure to air, the sample was separated by centrifuging. The transparent green solution was used to measure the double bond conversion by NMR spectrum and molecular weight by GPC; the black solid was washed with THF several times and dried in vacuum, affording a sample of hyperbranched glycopolymer-grafted MWNTs. Five experiments with different γ were conducted. The selected results are summarized in Table 2.

Deprotection. The transformation of linear or hyperbranched poly(3-*O*-methacryloyl-1,2:5,6-di-*O*-isopropylidene-D-glucopyranose)-grafted MWNTs (MWNT-g-polyMAIG) into poly(3-*O*-methacryloyl- α,β -D-glucopyranose)-grafted MWNTs (MWNT-g-polyMAG) was achieved under acidic conditions.⁵⁴ Typically, MWNT-g-polyMAIG (50 mg) was dispersed in 80% formic acid (20 mL) and stirred for 48 h at room temperature. Then 10 mL of water was added and the mixture was stirred for 12 h. The black solid product was then collected after several cycles of centrifuging and water washing.

Results and Discussion

I. Linear Glycopolymer-Grafted MWNTs. Synthesis. Glycopolymers are of interest because of their biocompatibility, high density of multihydroxyl groups, and water solubility.⁵⁵ Syntheses of neat linear glycopolymer and polymer brushes have

Table 2. Reaction Conditions and Results for the Self-Condensing Vinyl Copolymerization (SCVCP) of MAIG and BIEM in the Presence of MWNT-Br

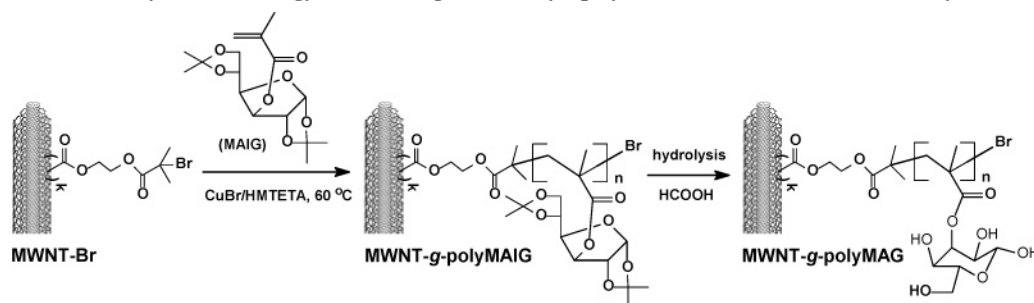
γ^a	time/h ^b	convn/% ^c	$M_{n,app}$ ^d	PDI ^d	$f_{wt}/\%$ ^e	MW _{TGA} ^f	DB _{NMR}	DB _{theo}
0	4.5	~95.0	4000	1.88	0.38	1165		0.465
0.5	21.5	73.8	3660	1.77	0.40	1270	0.49	0.50
1	4.5	~95.7	5630	2.03	0.42	1380	0.43	0.49
2.5	22.0	~93.0	4200	1.86	0.46	1680	0.34	0.40
5	29.5	~90.0	4370	1.81	0.53	2140	0.21	0.24

^a The feed mole ratio of MAIG to BIEM. ^b A sample is taken from the reaction system after a given time to determine the conversion by NMR. The final reaction time set is dependent on the conversion of vinyl groups and the viscosity of the reaction system. In the case of either quite high viscosity (so it is difficult to take a sample by the syringe from the reaction system) or the small conversion difference after a relatively long reaction time, the reaction would be stopped. The initial feed ratio of BIEM to ethyl acetate is approximately 1/2 ($\gamma = 0$), 1/5 ($\gamma = 0.5$), 1/2 ($\gamma = 1$), 1/2.5 ($\gamma = 2.5$), and 1/5 ($\gamma = 5$) g/mL. ^c The conversion of vinyl groups determined by ¹H NMR. ^d The apparent number-average molecular weight (M_n) and polydispersity index (PDI) of soluble polymer measured by GPC. ^e The polymer content grafted on MWNTs, determined by TGA. ^f The average molecular weight evaluated from TGA.

shown that polymerization of MAIG monomer can be well controlled by ATRP.^{54–56} It was reported that nanocarbons^{25,28} or other graphitic nanosurfaces⁵⁷ have different effects on ATRP compared to other surfaces, such as gold and silicon wafer or nanoparticles.⁵⁸ Herein, we graft glycopolymers from MWNTs to prepare biocompatible polymer-coated nanowires, and to examine the controllability for polymerization of MAIG in the presence of CNTs. Generally, two different ways can be used: initiation using only CNT-based macroinitiator (CNT-Br) or with both the macroinitiator and sacrificial initiator. In this article, we tried both ways to investigate the influence of sacrificial initiator on the controllability of the heterogeneous polymerization. The grafting efficiency of polymers on to the CNTs has been studied by changing the feed ratio of CNT-Br to monomer and block copolymerization in previous papers.^{27–32} However, the kinetics or the process was rarely investigated, especially for MWNTs.²⁴ Therefore, we focused on the kinetics and characterization of the products obtained at different reaction time, and omitted the feed ratio effect in this work. The synthetic steps of glycopolymer-grafted MWNTs are depicted in Scheme 1. PolyMAIG was grown from MWNTs by ATRP, followed by deprotection of the MAIG units, giving rise to multihydroxy MWNT-g-polyMAG.

Kinetics. In experiments where co-initiators of MWNT-Br and ethyl 2-bromoisobutyrate were used, the monomer conver-

Scheme 1. Synthetic Strategy for Grafting Linear Glycopolymer from Surfaces of MWNTs by ATRP



sions were obtained from ^1H NMR spectra of the samples taken from the reaction system with the peak of anisole at δ 6.6–6.8 ppm as the reference. The molecular weight and PDI of the soluble polymer were measured by GPC using PS standards. The grafted polymer fraction ($f_{\text{wt}}\%$) for the solid products of MWNT-g-polyMAIG was obtained from the corresponding TGA curves. The results are summarized in Table 1.

The first-order time–conversion plot is linear (see Figure 1a), and a linear relationship is obtained between monomer conversion and apparent molecular weight (see Figure 1b). These are in good agreement with kinetics of normal ATRP in a homogeneous system.⁵⁴ It is noteworthy that the PDI is rather low (<1.28) below ca. 45–50% of monomer conversion. After this conversion, however, the PDI increases with reaction time (see Table 1 and Figure 1b). From the GPC curves, a shoulder peak at lower elution volume appeared at 4.5 h (44.6% conversion) and became stronger with reaction time (see Figure 2). This can be assigned to the coupled polymer, as its molecular weight is twice as large compared to the main peak. Hence, the broader PDI after 45–50% conversion can be attributed to the

polymer coupling in the reaction system. In the control experiments without CNTs, no coupling peak was observed even at high conversion ($>80\%$). Therefore, coupling is more predominant for ATRP initiated by free initiator in the presence of the carbon-based macroinitiator. If the conversion at the appearance point of coupling is coined as “critical conversion of coupling” (CCC), the CCC for CNT surface-initiated ATRP is much lower than that of conventional homogeneous ATRP. This conclusion could be expanded to most of graphitic carbon surface-initiated polymerizations where polymer brushes have been obtained by using ATRP-active monomers.^{28,57} Obviously, the effect of carbon on ATRP is not negligible, compared with other surfaces such as silicon and gold.⁵⁸ This carbon effect is likely due to the unique electronic property of carbon. This phenomenon even needs further studies.

For the MWNT-g-polyMAIG, the content of grafted polymer increased from 38 to 71 wt % with increasing monomer conversion from 18.7% to ca. 85% (see Table 1 and Figure 3), implying that the polymer content can be adjusted over a wide range by monomer conversion or reaction time. Significantly, the average molecular weight (M_{TGA}) calculated from TGA results also increases linearly with the conversion, indicating that the kinetics for the polymerization initiated by MWNT-Br is almost same as that initiated by the sacrificial initiator, ethyl 2-bromoisobutyrate, in one reaction system. From the ratio of $M_{\text{TGA}}/M_{\text{n,theo}}$, the initiating efficiency (E_{ini}) of MWNT-Br can be evaluated assuming that E_{ini} of ethyl 2-bromoisobutyrate is 100%. It is found that E_{ini} of MWNT-Br is ca. 14–15%, corresponding to 0.9–1.0 polymer chains per 1000 carbons. In other words, because of the low initiating efficiency of MWNT-Br, M_{TGA} is much lower than $M_{\text{n,theo}}$ and $M_{\text{n,app}}$.

In order to confirm the aforementioned results, we conducted another experiment with the same conditions (data not shown), giving almost the same results and conclusions: (1) linear kinetics plot between conversion and molecular weight of free polymer and grafted polymer, (2) coupling at reaction time of

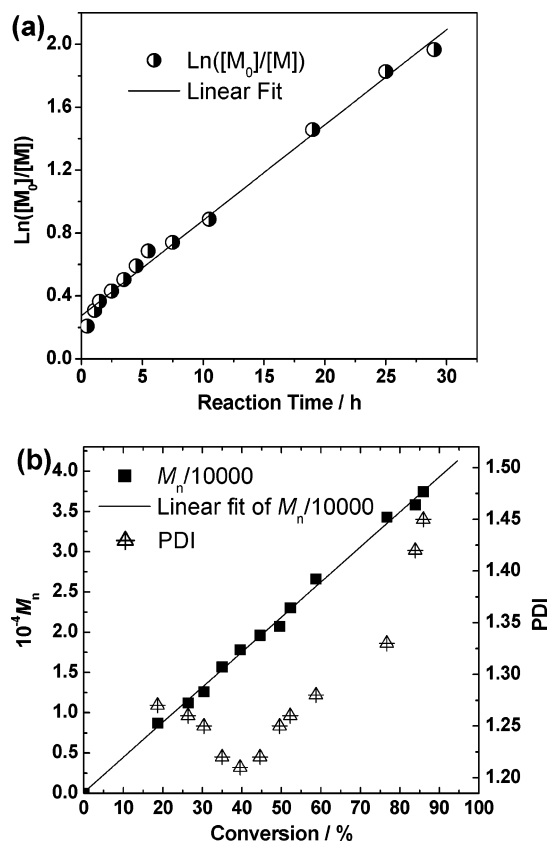


Figure 1. First-order time–conversion plot (a), and apparent number-average molecular weight (M_n) and polydispersity index (PDI) of the soluble polymer as a function of monomer conversion (b).

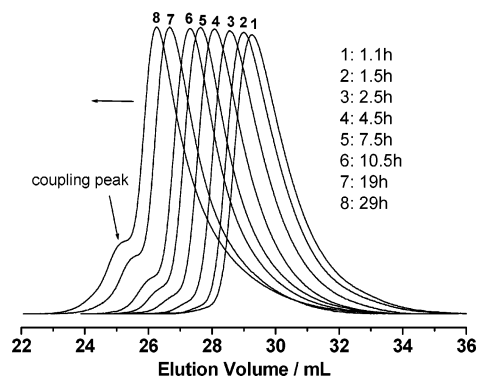


Figure 2. Selected GPC curves of the nongrafted polymer initiated by MWNT-Br and ethyl 2-bromoisobutyrate.

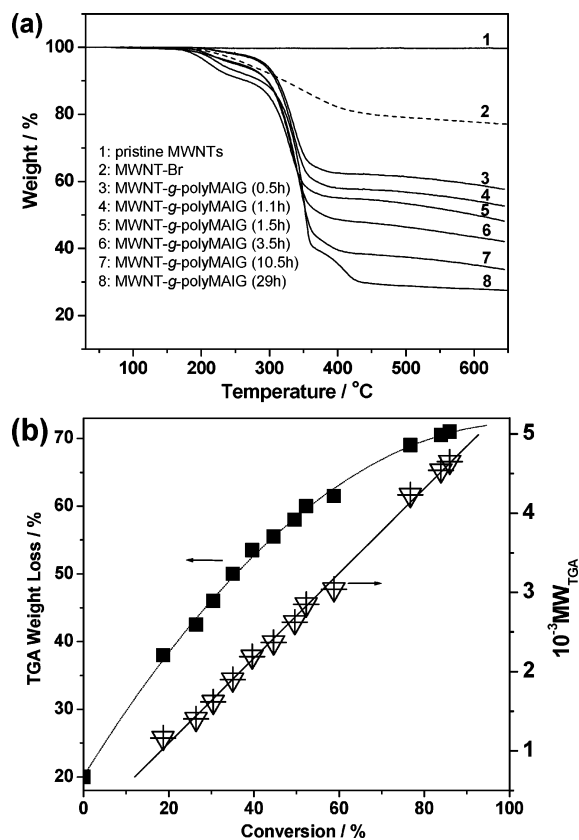


Figure 3. TGA weight loss curves for the pristine MWNTs, MWNT-Br, and linear glycopolymer-grafted MWNTs obtained at different reaction time (a), and the content and average molecular weight of the polymer grafted onto MWNTs, calculated from corresponding TGA data, as a function of monomer conversion (b).

4.5–5.5 h or monomer conversion of 45–50%, (3) PDI increased with the conversion after CCC (ca. 45–50%).

In order to compare, the polymerization initiated with MWNT-Br in the absence of sacrificial initiator was also conducted. Again, a linear plot between MW_{TGA} and conversion was observed for the case of MWNT-Br (data not shown). Furthermore, almost the same grafting efficiency as the case of co-initiators was achieved. After 25 h, the content of grafted polymer was 71.5 wt %. These results confirm that the kinetics for the ATRP of MAIG initiated by MWNT-Br alone is comparable to that obtained in the presence of sacrificial initiator.

NMR and FTIR Spectra. The chemical structure of the resulting MWNT-g-polyMAIG was also characterized by NMR and FTIR. In the 1H NMR spectrum (Figure 4a), the peaks of polyMAIG moiety are found clearly at δ 0.5–2.2 ppm (CH_3- , $-CH_2-$), 3.8–5.0 ppm ($-CH_2O-$, $-CHO-$), 5.8 ppm ($-CHO-$). In the FTIR spectra (Figure 5a), strong absorption peak of carbonyl group was observed at 1731 cm^{-1} , and the peaks assigned to methyl and ethylene units were found at 2800 – 3100 cm^{-1} . The higher the f_{wt} %, the stronger the absorption peak.

Deprotection. After deprotection of the MWNT-g-polyMAIG in 80% formic acid, multihydroxy MWNT-g-polyMAG were obtained. In the 1H NMR spectrum of MWNT-g-polyMAG (Figure 4b), the peak assigned to isopropylidene groups disappeared, the peak of $-CHO-$ (J) shifted from 5.8 to 6.8 ppm, and the peak of anomeric hydroxyl group appeared at 8.2 ppm. In the FTIR spectrum (Figure 5a), the absorption peaks at 2800 – 3100 cm^{-1} became weaker and the peak of hydroxyl group at 3450 cm^{-1} became stronger due to the cleavage of CH_3- groups

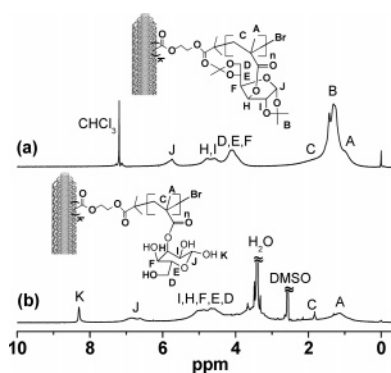


Figure 4. 1H NMR spectra of linear glycopolymer-grafted MWNTs in $CDCl_3$ (a) and deprotected glycopolymer-grafted MWNTs in $DMSO-d_6$ (b).

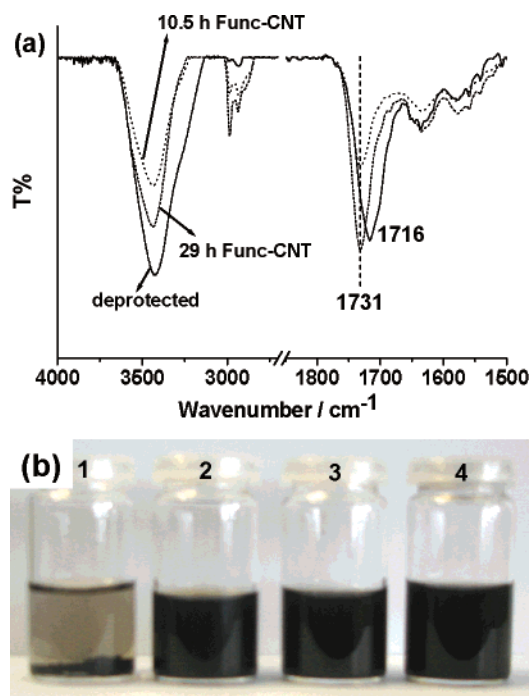


Figure 5. (a) FTIR spectra of linear glycopolymer-grafted MWNTs obtained at 10.5 and 29 h and deprotected glycopolymer-grafted MWNTs at 29 h. (b) Photographs of pristine MWNTs in THF, precipitating at the bottom (1), linear glycopolymer-grafted MWNTs at 29 h in THF (2), deprotected glycopolymer-grafted MWNTs at 29 h in water (3), and hyperbranched glycopolymer-grafted MWNTs with $\gamma = 1$ in THF (4). The photographs were taken after the samples were dispersed in corresponding solvents and sonicated for ca. 2 min and then allowed to stand for a day.

and formation of hydroxyl groups, and the vibration of carbonyl group shifted to 1716 cm^{-1} . The MWNT-g-polyMAIG can be well dispersed in apolar and weakly polar solvents such as chloroform, ethyl acetate, and THF. After deprotection, the MWNT-g-polyMAG are not soluble in nonpolar solvents but soluble in highly polar solvents such as water, methanol, DMSO, and DMF. Figure 5b shows photographs of pristine and polymer-functionalized MWNTs in solvents.

SEM, TEM, and SFM Observations. The morphology and nanostructures of the resulting products were observed by SEM, TEM, and SFM. Figure 6 shows the representative SEM images and as it can be seen that oxidized MWNTs (MWNT-COOH) (Figure 6a) and MWNT-Br (Figure 6b) exhibit nanowire-like morphology. For the MWNT-g-polyMAIG collected at 3.5 h (Figure 6c, 53.5 wt % polymer), a nanowire-like morphology can also be observed, but the space among nanowires becomes smaller. For the sample obtained after 10.5 h (Figure 6d, 61.5

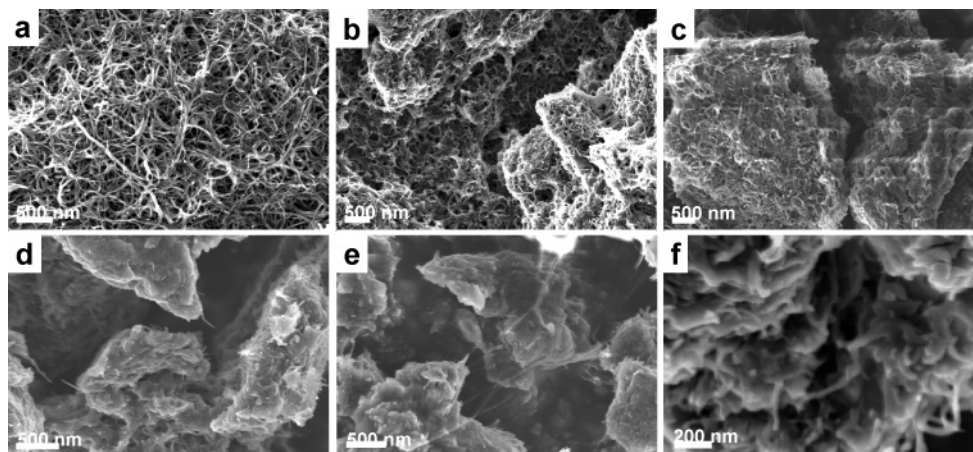


Figure 6. Representative SEM images of oxidized MWNTs (a), MWNT-Br (b), linear glycopolymer-functionalized MWNTs at 3.5 (c), 10.5 (d), and 29 h (e), and the deprotected glycopolymer-functionalized MWNTs at 29 h (f).

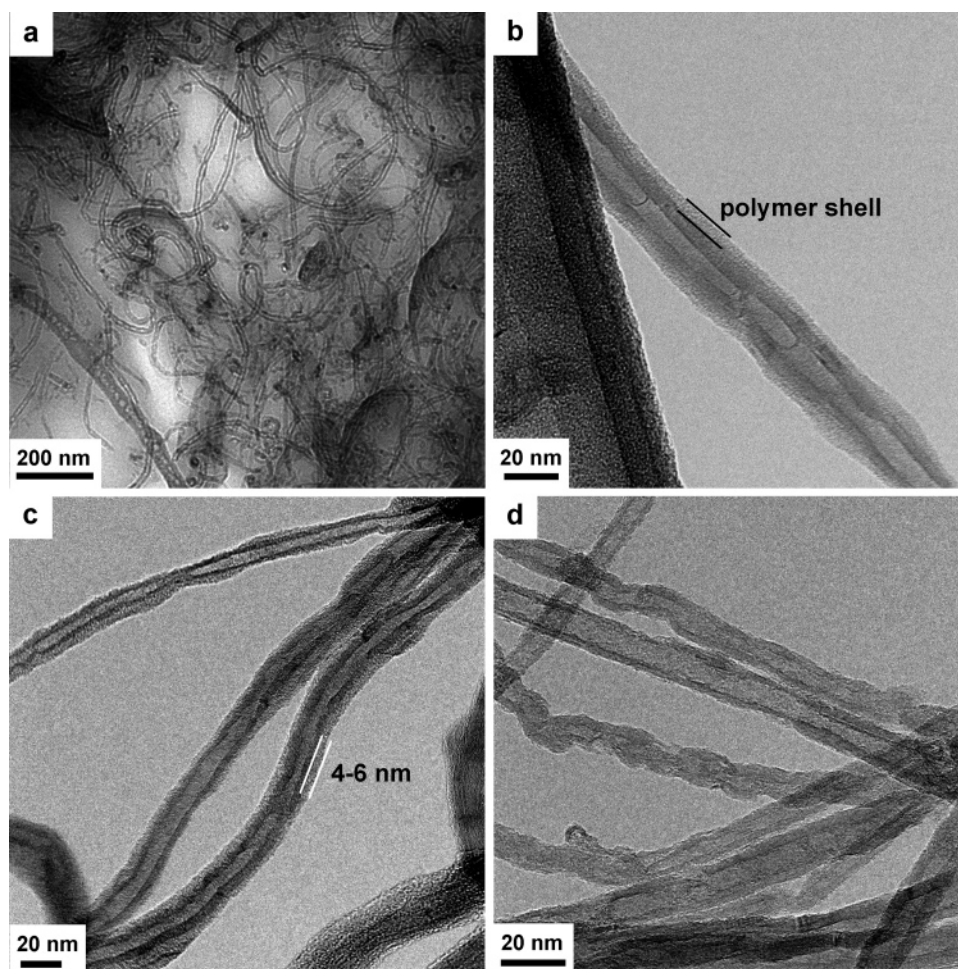


Figure 7. Representative TEM images of linear glycopolymer-functionalized MWNTs at 29 h (a) and 10.5 h (b), deprotected glycopolymer-functionalized MWNTs at 29 h (c), and MWNT-Br (d).

wt % polymer), a continuous polymer phase is observed, and a nanowire-like structure cannot be clearly observed. For the sample obtained after 29 h (Figure 6e, 71 wt % polymer), only a continuous phase can be observed, and straight fiberlike structures can be found between two big structures. These observations confirm that the polymer content in the product increases with the reaction time. After deprotection, a diffuse nanowire-like morphology can be observed indistinctly (Figure 6f), indicating that the polymer content became lower due to the cleavage of the protected units.

The resulting products were also characterized by TEM. When the polymer content is high, the MWNT-g-polyMAIG can form a self-standing film on the TEM grid (see Figure 7a). In this film, CNTs were well dispersed, resembling CNTs-reinforced polymer nanocomposites. For the sample obtained after 10.5 h, the core-shell structure of polymer layer-coated CNTs can be distinctly observed under high magnification (Figure 7b). After deprotection of the sample obtained after 29 h, a core-shell structure with 4–6 nm of polymer shell can also be clearly observed (Figure 7c), indicating the polymer

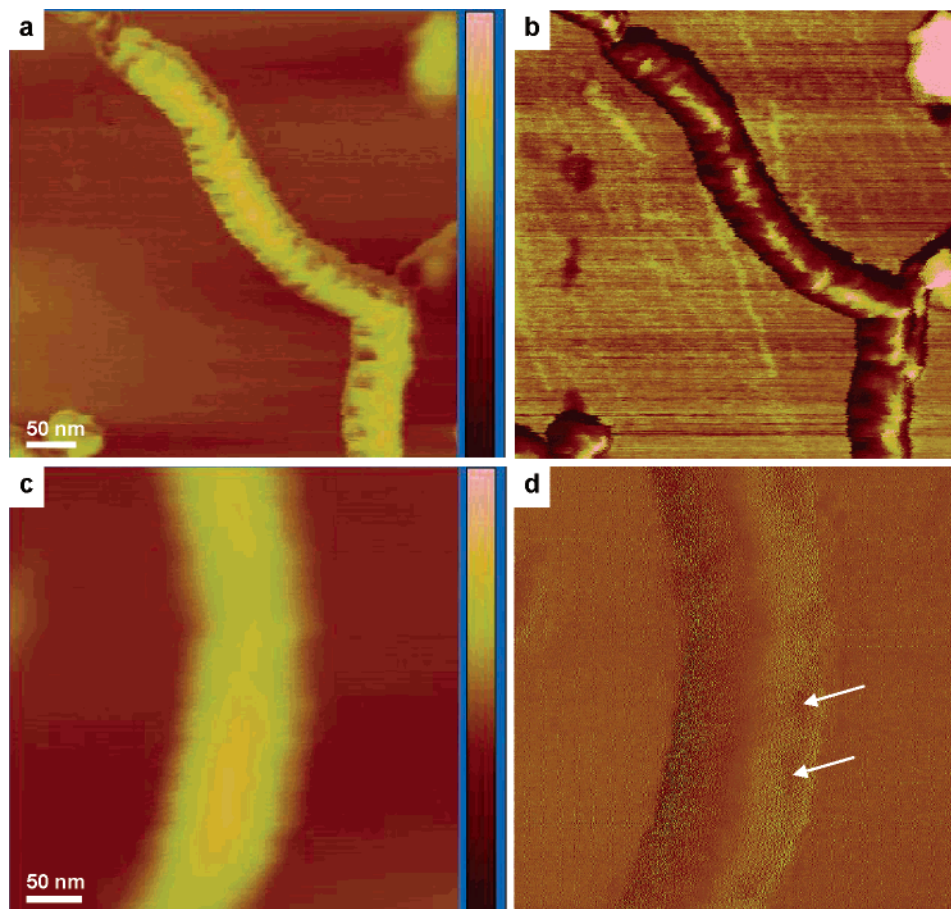


Figure 8. Representative height (left) and phase (right) SFM images of MWNT-Br (a, b) and linear glycopolymer-functionalized MWNTs at 29 h (c, d). The color height bars represent 50 (a) and 100 nm (c), respectively.

remains grafted on the surface of the CNTs. For the MWNT-Br, no core-shell structure was observed (Figure 7d). These observations are in agreement with those reported before for other polymer-functionalized MWNTs, wherein similar core-shell structure was formed when certain amount of polymer was grafted onto MWNTs, and a self-standing film was also observed when the grafted polymer content was high.^{23,28}

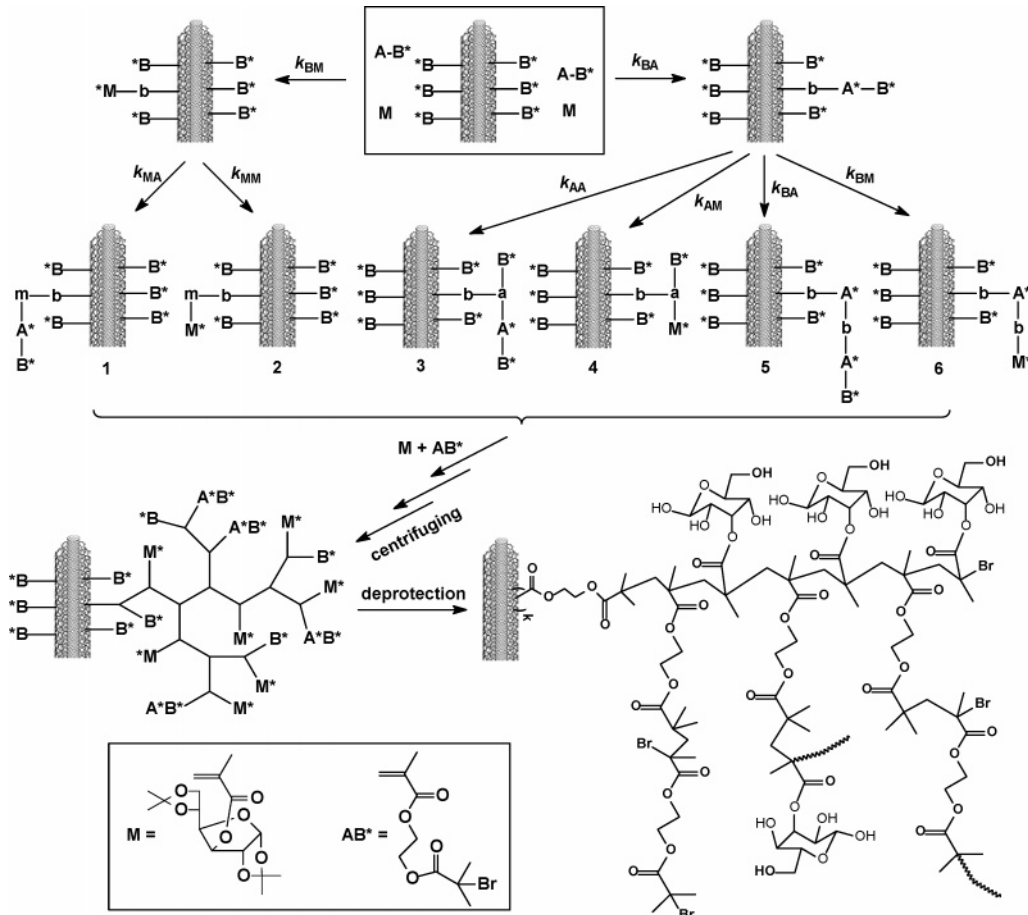
It is known that scanning force microscopy (SFM) is a powerful tool to detect individual polymer brushes. Herein, we have also employed SFM for the characterization of CNT-based cylindrical polymer brushes. For the MWNT-Br, a cylindrical nanowire-like morphology was clearly observed in both height and phase images (Figure 8, a and b). For the sample with high content of polymer (Figure 8, parts c and d), different morphology was found: (1) the width (ca. 122 nm) of the tube is obviously larger than its height (ca. 35 nm), (2) a high density of fuzzy structure is observed in the height image, and (3) a collapsed or compressed structure is found in the phase image, as denoted by the arrows. These differences imply that polymer chains are grafted on MWNTs at high density, forming nanotube-supported polymer brushes.

II. Hyperbranched Glycopolymer-Grafted MWNTs. Hyperbranched glycopolymer was grafted from MWNTs by self-condensing vinyl copolymerization (SCVCP) of MAIG monomer and BIEM AB* inimer. In fact, SCVCP is an advanced approach of self-condensing vinyl polymerization (SCVP) since common ATRP-active vinyl monomers such as methyl methacrylate and styrene can be employed to build up hyperbranched polymers with the incorporation of inimer units.⁵⁹ Recently, Hong and co-workers grafted hyperbranched polymers from MWNTs with high efficiency by SCVP using 2-((bromobu-

tyryl)oxy)ethyl acrylate (BBEA) as the inimer.⁴⁶ The SCVCP of BBEA and *tert*-butyl acrylate was also tried successfully, but detailed characterizations were not reported.⁴⁶ The kinetics of polymerization, DB, the degree of branching, and other important molecular parameters of hyperbranched polymers such as molecular weight and PDI were also not investigated and evaluated. These problems will be addressed with the model SCVCP of MAIG and BIEM below.

Synthesis. Scheme 2 illustrates the reaction steps and initiating mechanism for SCVCP of inimer (AB*) and monomer (M). In the presence of catalyst, the CNT-Br is activated as CNT-B*. The CNT-B* can initiate the polymerization of AB* and M. Addition of one unit of AB* or M to CNT-B* results in the formation of CNT-*b*-A*B* or CNT-*b*-M*. Then, both CNT-*b*-A*B* and CNT-*b*-M* react with M and AB*, giving rise to species of 1-6 shown in Scheme 2. At the same time, AB* in the solution initiates the reaction of M and AB* itself. The six activated species of macroinitiators (1-6) and corresponding activated species forming from the reactions of AB* and M further initiate polymerizations of AB*, M and the formed oligomers, affording hyperbranched glycopolymer-grafted MWNTs and free hyperbranched polymer. After centrifuging, solid products of functionalized CNTs and solution of the free hyperbranched polymer were obtained separately. According to previous studies, we selected (PPh₃)₂NiBr₂ as the catalyst and 100 °C as the reaction temperature.^{56,60} In addition to the SCVP of neat BIEM ($\gamma = 0$), copolymerizations with four different monomer/inimer ratios ($\gamma = 0.5, 1, 2.5, \text{ and } 5$) were tried. The grafted polymer content and other results are summarized in Table 2.

Scheme 2. Synthetic Strategy for Grafting Hyperbranched Glycopolymer from Surfaces of MWNTs by Self-Condensing Vinyl Copolymerization (SCVCP) of Inimer (AB^*) and Monomer (M) via ATRP



The content of the grafted hyperbranched copolymer is 38–53 wt %, which is lower than that of linear polymer. This is likely attributed to the relatively lower E_{ini} of MWNT–Br and cyclization of soluble hyperbranched macromolecules during the SCVCP as compared to the case of linear polymer grafting. Such lower E_{ini} is possibly related to the polymerization mechanism of SCVP or SCVCP. In SCVP between monomers, oligomers and macromolecules occur simultaneously. Once the inimer molecules are initiated and reacted, condensations among oligomers and macromolecules became predominant reactions, resulting in less grafting efficiency on the solid surface than in the solution because of strong steric hindrance between macromolecules. Another possible reason is cyclization of hyperbranched polymers. After cyclization, there is no A functional group in the macromolecule any more, making the reaction between the macromolecule and the B groups on the carbon nanotube impossible.

Kinetics. Figures 9 and 10 show the kinetic plots and GPC curves in the cases of $\gamma = 1$ and 0.5. The apparent molecular weights and PDI of the free polymer increase with conversion of vinyl groups. In the GPC curves, shoulder peaks can be observed after ca. 50% conversion (see Figures 9a and 10a). Therefore, the relationship between peak molecular weight (M_p) and conversion is also shown in the figures. For the two cases ($\gamma = 1$ and 0.5), the increasing tendency of molecular weight and PDI is in consistent with the theory prediction.^{61,62}

On the other hand, we found that the apparent M_n leveled off after certain conversion (ca. 90%) in the cases of $\gamma = 2.5$ and 5 (see Table 3). This is possibly caused by the different DB of hyperbranched copolymer at different conversion.

Theoretically, higher the conversion, greater would be the DB.^{62,63} In addition, cyclization of the macromolecules may also influence the apparent molecular weight.

NMR Spectra and DB.⁶⁰ The resulting products of hyperbranched polyMAIG-grafted MWNTs were characterized by NMR, as shown in Figure 11. For the case of $\gamma = 0$, the hydrogen peaks of polyBIEM units such as CH_3- , $-CH_2-$, CH_3-C-Br , and $-CH_2O-$ are observed at δ 0.5–1.25, 1.55–1.9, 1.92, and 4.0–4.5 ppm. For the copolymer-grafted MWNTs, the peaks of both polyBIEM and polyMAIG units are also found in corresponding NMR spectrum (see Figure 11). For instance, The characteristic peaks of polyMAIG units are clearly seen at 1.2–1.4 ppm (isopropylidene protons), 3.8–5.0, and 5.7–6.0 ppm. It is noteworthy that the integration ratio of the isopropylidene protons of polyMAIG to the methyl protons adjacent to a bromine atom (CH_3-C-Br , A^* and M^* in the polymer chain end and B^* in the 2-bromoisobutyryloxy group) increases with increasing the γ , which is well consistent with the feed ratio of MAIG to BIEM. Apart from these peaks, a peak b formed by addition of the monomer to B^* should be observed at around 0.8–1.4 ppm. However, peak b is invisible in the spectrum, because it is overlapping with the isopropylidene protons of the polyMAIG segments and the methyl protons of the polymer backbone. From the 1H NMR spectra, the MAIG content in the grafts of hyperbranched copolymer can be determined by comparing the peak at 5.7–6.0 ppm corresponding to one proton (K) of the polyMAIG segments with the peaks at 3.8–5.0 ppm, attributed to the sum of six protons (E, H, I, J, G) of the polyMAIG segments and four protons of ethyleneoxy units ($-OCH_2CH_2O-$) of the polyBIEM segments.

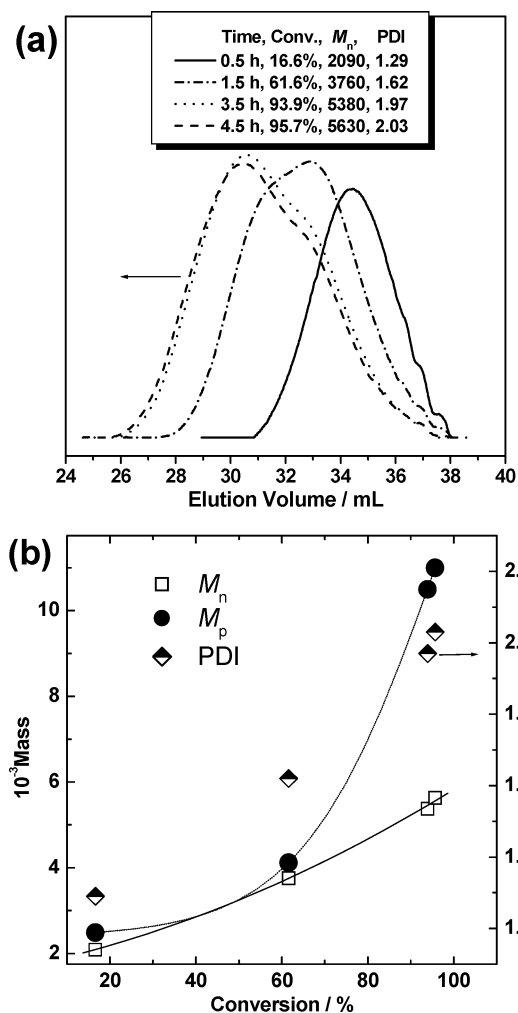


Figure 9. GPC curves of the free hyperbranched polymer collected from the self-condensing vinyl copolymerization system of MAIG and BIEM with $\gamma = 1$ at different conversion or reaction times (a) and the corresponding molecular weight and PDI of the polymer as a function of conversion (b).

Thus, the composition of the two segments can be calculated using eq 1,

$$\frac{6H(x) + 4H(1-x)}{1H(x)} = \frac{\text{integral at 3.8–5.0 ppm}}{\text{integral at 5.7–6.0 ppm}} \quad (1)$$

where x is the fraction of the monomer and $1-x$ is the fraction of the inimer in the copolymer. The comonomer fractions calculated from the ratio of these peaks are in good agreement with the feed ratio γ .

DB of the hyperbranched glycopolymers grafted onto CNTs were also evaluated using ^1H NMR, since DB is an important parameter for hyperbranched polymers. The direct determination of DB by NMR for hyperbranched methacrylates obtained by SCVP of methacrylate-type inimers via ATRP is quite difficult. For neat polyBIEM, the proportion of B^* and b cannot be determined directly, because of the overlapping signals of the methyl protons in the polymer backbone with the methyl protons from the B^* and b groups.⁶⁴ In cases of the copolymers obtained by SCVCP, these peaks (B^* and b) are related to DB and the comonomer composition. The fraction of B^* units could be calculated by comparing the peaks at 3.8–5.0 ppm and peak around 1.9–2.0 ppm in the copolymers ranging from $\gamma = 1$ to $\gamma = 10$. The peaks at 3.8–5.0 ppm correspond to six protons of polyMAIG segment and four protons of polyBIEM segment,

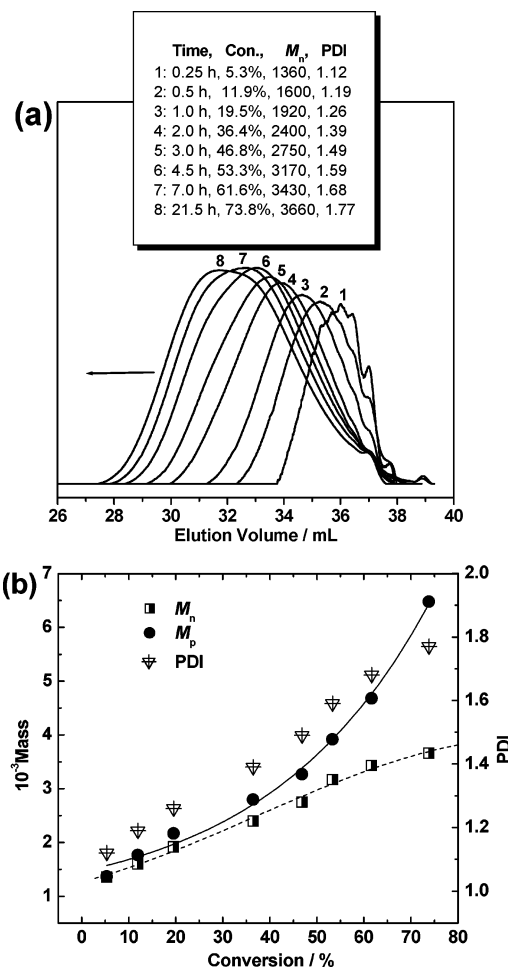


Figure 10. GPC curves of the free hyperbranched polymer collected from the self-condensing vinyl copolymerization system of MAIG and BIEM with $\gamma = 0.5$ at different conversion or reaction times (a) and the corresponding molecular weight and PDI of the polymer as a function of conversion (b).

Table 3. Kinetic Investigations and Results for the Self-condensing Vinyl Copolymerization (SCVCP) of MAIG and BIEM with γ 2.5 and 5 in the Presence of MWNT-Br via ATRP.

γ	time/h	convn/% ^a	$M_{n,\text{app}}^b$	PDI ^b	$M_{p,\text{app}}^c$
2.5	0.5	31.6	2240	1.30	2500
	1.0	55.7	3370	1.50	3520
	1.5	77.8	3950	1.63	4100
	2.5	85.2	4500	1.78	8000
	3.5	89.5	4580	1.84	8030
	5.0	91.5	4550	1.85	8090
	7.5	92.9	4500	1.85	8110
	22.0	~93.0	4200	1.86	7580
5.0	0.5	18.3	2040	1.24	2320
	1.5	58.9	3740	1.53	4000
	2.5	76.4	4610	1.67	7100
	3.5	86.1	4710	1.73	7700
	5.0	~87.0	4760	1.76	7900
	7.0	~87.0	4690	1.78	7700
	20.5	~87.0	4410	1.80	7370
	29.5	~90.0	4370	1.81	7140

^a The conversion of vinyl groups determined by ^1H NMR. ^b The apparent number-average molecular weight (M_n) and polydispersity index (PDI) of soluble polymer measured by GPC using linear PS standards. ^c The apparent peak molecular weight.

as mentioned above. The peak at 1.9–2.0 ppm corresponds to methyl protons adjacent to a bromine atom (A^* and M^* in the polymer chain end and B^* in the 2-bromoisobutyryloxy group). B^* in BIEM is consumed during the copolymerization, and consumption of one B^* would lead to formation of one A^* or

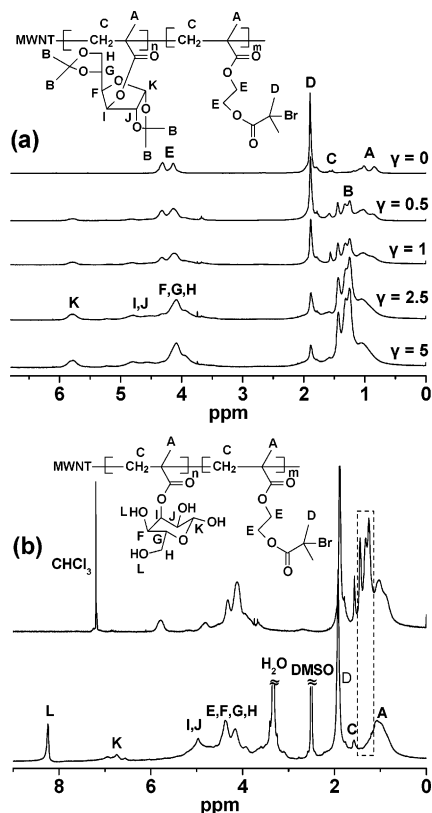


Figure 11. ^1H NMR spectra of the hyperbranched glycopolymer-functionalized MWNTs with different γ in CDCl_3 (a), and the deprotected hyperbranched glycopolymer-functionalized MWNTs with $\gamma = 1$ in $\text{DMSO}-d_6$ (b, bottom spectrum; the upper spectrum is the corresponding protected precursor with $\gamma = 1$).

M^* , and consequently, original $B^* = B^*_{\text{left}} + A^* + M^*$. B^*_{left} corresponds to six protons, whereas $A^* + M^*$ has three protons. Once the fractions of the monomer x and the inimer $1 - x$ in the copolymer are known (see eq 1), the value of B^* can be calculated from eq 2,

$$\frac{6H(x) + 4H(1-x)}{6H(B^*) + 3H(1-x)} = \frac{\text{integral at } 3.8 - 5.0 \text{ ppm}}{\text{integral at } 1.9 - 2.0 \text{ ppm}} \quad (2)$$

Since $B^* + b = 1$, b can also be ascertained. Hence, we can indirectly calculate the proportion of b using ^1H NMR, and then evaluate DB. For equal reactivity of active sites, DB determined by NMR (DB_{NMR}) at full conversion is given as the eq 3,⁶²

$$\text{DB}_{\text{NMR}} = 2\left(\frac{b}{\gamma + 1}\right)\left[1 - \left(\frac{b}{\gamma + 1}\right)\right] \quad (3)$$

According to the theory of SCVCP,⁶² DB_{theo} , at full conversion, can be represented as the eq 4,

$$\text{DB}_{\text{theo}} = \frac{2(1 - e^{-(\gamma+1)})(\gamma + e^{-(\gamma+1)})}{(\gamma + 1)^2} \quad (4)$$

For instance, $\text{DB}_{\text{NMR}} = 0.43$ and $\text{DB}_{\text{theo}} = 0.49$ can be obtained at $\gamma = 1$ ($b = 0.62$). Other values of DB are listed in Table 2. DB decreases from 0.49 to 0.21 as γ increases from 0.5 to 5. The decreasing tendency is in agreement with theory. DB_{NMR} is somewhat smaller than the corresponding DB_{theo} , which could be attributed to (1) the simplifications made for the calculations, i.e., equal reactivity of A^* , B^* , and M^* chain ends, and (2) the full conversion assumption.

Deprotection. The same protocol as the deprotection of linear MWNT-g-polyMAIG was employed to deprotect the hyperbranched glycopolymer-grafted MWNTs in formic acid.^{56,60} In the ^1H NMR spectrum of the deprotected product, the isopropylidene protons of polyMAIG segments were not observed, and proton of hydroxyl groups was seen at 8.3 ppm. One peak (K) shifted from 6.0 to 6.8 ppm, because of the change of structure, as shown in Figure 11b. In addition, the unchanged resonance signal of protons of the ethylene linkage at 4.0–4.6 ppm suggests that the branched structure is intact during the complete deprotection of the isopropylidene groups, and the polyBIEM segment is almost same as that before deprotection. The as prepared products can be well dispersed in weakly polar or apolar solvents such as THF, chloroform, ethyl acetate (a photograph is shown in Figure 5b). After deprotection, the solubility or dispersibility was dependent upon the comonomer ratios, γ . For the cases of $\gamma = 0.5$ or 1, hyperbranched glycopolymer-grafted MWNTs can be dispersed in both polar solvents such as methanol, DMSO and water partially and weakly polar solvents such as acetone and THF because of the nonpolar inimer segment. For the cases of $\gamma = 2.5$ or 5, the resulting products can be well dispersed in strongly polar solvents, such as water, DMSO, and methanol, but relatively poorly dispersed in weakly polar solvents, such as THF and acetone.

TEM and SFM Observations. The resulting hyperbranched glycopolymer-grafted MWNTs were also characterized by TEM and SFM. The representative images are shown in Figure 12. As can be seen from TEM images, a polymer layer can also be observed on the surface of MWNT (Figure 12, parts b and d), implying that hyperbranched polymer has grown on the surfaces of CNTs uniformly. Compared with the MWNT-Br (Figure 12, parts a and b), a different morphology was also observed in the SFM images, especially in the phase images, the nanotubes assemble adhering to the mica tightly with a contour of polymer phase (see Figure 13 a and b), as denoted by the arrows. These TEM and SFM observations confirm the hyperbranched glycopolymer is successfully covalently grafted from MWNTs.

Conclusions

Linear glycopolymer was grafted from surfaces of MWNTs by ATRP. Kinetic investigation of the polymerizations with and without sacrificial initiator revealed that the content of polymer grafted on MWNTs increased with conversion of monomer or reaction time. The molecular weight of free polymer initiated by the sacrificial initiator also increased with the conversion of monomer linearly, indicating the kinetics of the heterogeneous polymerization is almost the same as conventional homogeneous polymerization. However, the critical conversion of coupling (CCC) is ca. 45–50% for the heterogeneous polymerization, which is much lower than that of homogeneous polymerization (>80%). The lower CCC implies that coupling occurs more easily in the carbon-surface initiated ATRP due to the unique property of the carbon surface. After deprotection in formic acid, water-soluble multihydroxy glycopolymer-grafted MWNTs were achieved. FTIR, NMR, TEM, SEM, and SFM confirmed the chemical structure and morphology of the resulting products. Because of the uniform and high density of grafting, a core-shell structure with MWNT as the core and polymer layer as the shell was observed.

Hyperbranched glycopolymers were also grafted from MWNTs by self-condensing vinyl copolymerization (SCVCP) of MAIG monomer and BIEM inimer via ATRP. The grafting efficiency

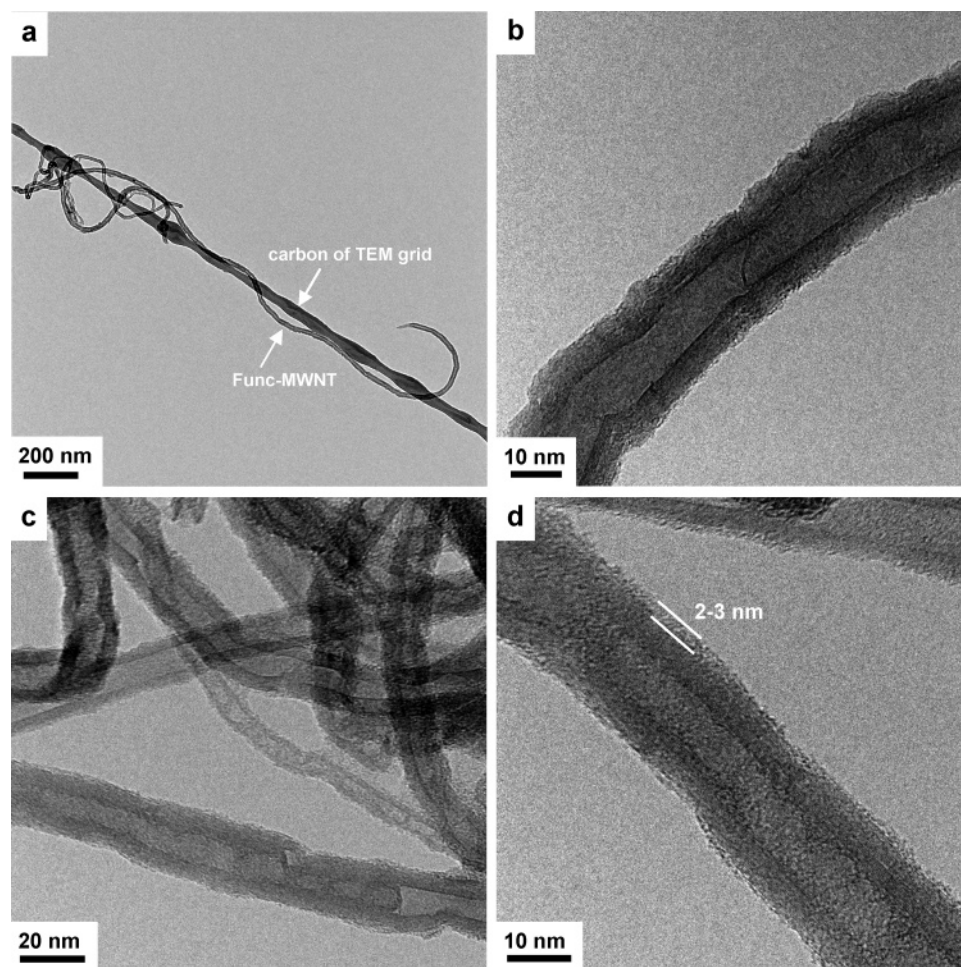


Figure 12. Representative TEM images of hyperbranched glycopolymer-functionalized MWNTs with $\gamma = 1$ (a, b) and 5 (c, d).

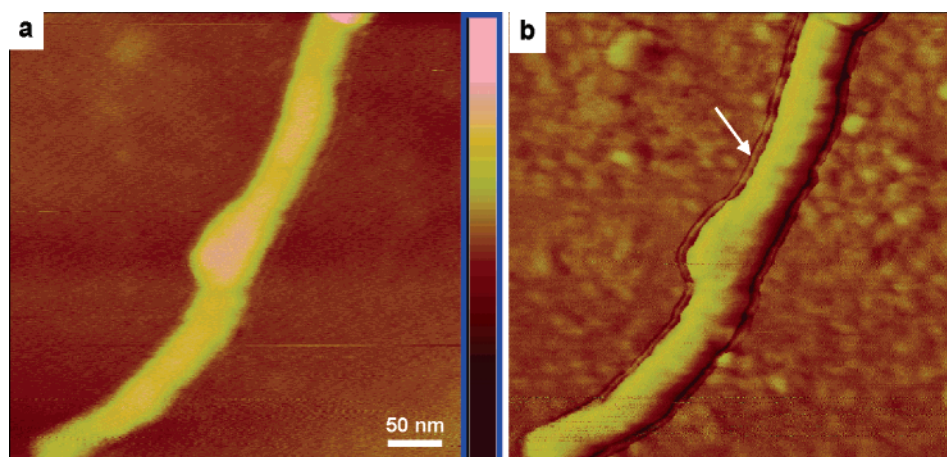


Figure 13. Representative height (left) and phase (right) SFM images of hyperbranched glycopolymer-functionalized MWNTs with $\gamma = 1$. The color height bars represent 40 nm.

is lower than the cases of linear glycopolymer. The degree of branching, DB, of the polymer grafted from MWNTs, evaluated by ^1H NMR, ranged from 0.49 to 0.21 when the monomer/inimer ratio, γ , increased from 0.5 to 5, in agreement with the theoretical prediction. Kinetic studies were carried out for SCVCP with different γ values. In the cases of lower γ (0.5 and 1), the apparent molecular weight and PDI increased with conversion; in the cases of higher γ (2.5 and 5), the molecular weight also increased with conversion at the beginning, and leveled off after certain conversion (ca. 90%). After deprotection, multihydroxy hyperbranched glycopolymer-grafted MWNTs

were obtained. The structure and morphology of the resulting products were characterized by NMR, TEM and SFM. In the TEM images, a core-shell structure was also observed. In SFM images, the HPGs-functionalized MWNTs assembly sticking to the mica surface with a contour of polymer phase was observed.

Because of the fact that linear and hyperbranched glycopolymers are biocompatible and the multihydroxy glycopolymers are water-soluble, the resulting polymer-functionalized MWNTs offer a versatile toolbox for applications in bionanotechnology.

Acknowledgment. This work was supported by the National Natural Science Foundation of China (Nos. 50473010 and 20304007), the Program for New Century Excellent Talents in University of China, the Foundation for the Author of National Excellent Doctoral Dissertation of China (No. 200527), Fok Ying Tung Education Foundation (No. 91013), and Deutsche Forschungsgemeinschaft (Grant No. Mu 896/14). C.G. thanks the Alexander von Humboldt Foundation (Germany) for granting a research fellowship.

References and Notes

- (1) (a) Iijima, S. *Nature (London)* **1991**, *354*, 56–58. (b) Iijima, S.; Ichihashi, T. *Nature (London)* **1993**, *363*, 603–605.
- (2) (a) Liu, J.; Rinzler, A. G.; Dai, H. J.; Hafner, J. H.; Bradley, R. K.; Boul, P. J.; Lu, A.; Iverson, T.; Shelimov, K.; Huffman, C. B.; Rodriguez-Macias, F.; Shon, Y. S.; Lee, T. R.; Colbert, D. T.; Smalley, R. E. *Science* **1998**, *280*, 1253–1256. (b) Chen, J.; Hamon, M. A.; Hu, H.; Chen, Y.; Rao, A. M.; Eklund, P. C.; Haddon, R. C. *Science* **1998**, *282*, 95–98.
- (3) Relevant reviews, for example, see: (a) Tasis, D.; Tagmatarchis, N.; Bianco, A.; Prato, M. *Chem. Rev.* **2006**, *106*, 1105–1136. (b) Hirsch, A.; Vostrowsky, O. *Top. Curr. Chem.* **2005**, *245*, 193–237. (c) Ajayan, P. M. *Chem. Rev.* **1999**, *99*, 1787–1799. (d) Dai, H. *Acc. Chem. Res.* **2002**, *35*, 1035–1044. (e) Szeleifer, I.; Yerushalmi-Rozen, R. *Polymer* **2005**, *46*, 7803–7818.
- (4) For relevant reviews, for example, see: (a) Lin, Y.; Taylor, S.; Li, H.; Fernando, S.; Qu, L.; Wang, W.; Gu, L.; Zhou, B.; Sun, Y.-P. *J. Mater. Chem.* **2004**, *14*, 527–541. (b) Sun, Y.-P.; Fu, K.; Lin, Y.; Huang, W. *Acc. Chem. Res.* **2002**, *35*, 1096–1104. (c) Niyogi, S.; Hamon, M. A.; Hu, H.; Zhao, B.; Bhowmik, P.; Sen, R.; Ikkis, M. E.; Haddon, R. C. *Acc. Chem. Res.* **2002**, *35*, 1105–1113. (d) Wang, C. C.; Guo, Z. X.; Fu, S. K.; Wu, W.; Zhu, D. B. *Prog. Polym. Sci.* **2004**, *29*, 1079–1141.
- (5) For example, see: (a) Sano, M.; Kamino, A.; Okamura, J.; Shinkai, S. *Langmuir* **2001**, *17*, 5125–5128. (b) Kahn, M. G. C.; Banerjee, S.; Wong, S. S. *Nano Lett.* **2002**, *2*, 1215–1218. (c) Huang, W.; Fernando, S.; Allard, L. F.; Sun, Y.-P. *Nano Lett.* **2003**, *3*, 565–568. (d) Lin, Y.; Zhou, B.; Fernando, K. A. S.; Allard, L. F.; Sun, Y.-P. *Macromolecules* **2003**, *36*, 7199–7204.
- (6) Li, H. M.; Cheng, F. O.; Duft, A. M.; Adronov, A. *J. Am. Chem. Soc.* **2005**, *127*, 14518–14524.
- (7) Kong, H.; Luo, P.; Gao, C.; Yan, D. *Polymer* **2005**, *46*, 2472–2485.
- (8) (a) He, P. G.; Bayachou, M. *Langmuir* **2005**, *21*, 6086–6092. (b) Qin, S. H.; Qin, D. Q.; Ford, W. T.; Zhang, Y. J.; Kotov, N. A. *Chem. Mater.* **2005**, *17*, 2131–2135. (c) Zhang, M. N.; Yan, Y. M.; Gong, K. P.; Mao, L. Q.; Guo, Z. X.; Chen, Y. *Langmuir* **2004**, *20*, 8781–8785. (d) Artyukhin, A. B.; Bakajin, O.; Stroeve, P.; Noy, A. *Langmuir* **2004**, *20*, 1442–1448.
- (9) For example, see: (a) Bahun, G. J.; Wang, C.; Adronov, A. *J. Polym. Sci., Part A: Polym. Chem.* **2006**, *44*, 1941–1951. (b) Martin, R. B.; Qu, L. W.; Lin, Y.; Harruff, B. A.; Bunker, C. E.; Gord, J. R.; Allard, L. F.; Sun, Y. P. *J. Phys. Chem. B* **2004**, *108*, 11447–11453. (c) Qu, L. W.; Martin, R. B.; Huang, W. J.; Fu, K. F.; Zweifel, D.; Lin, Y.; Sun, Y. P.; Bunker, C. E.; Harruff, B. A.; Gord, J. R.; Allard, L. F. *J. Chem. Phys.* **2002**, *117*, 8089–8094. (d) Petrov, P.; Stassin, F.; Pagnouille, C.; Jerome, R. *Chem. Commun.* **2003**, 2904–2905. (e) Gomez, F. J.; Chen, R. J.; Wang, D. W.; Waymouth, R. M.; Dai, H. J. *Chem. Commun.* **2003**, 190–191.
- (10) (a) Liu, Y. Q.; Yao, Z. L.; Adronov, A. *Macromolecules* **2005**, *38*, 1172–1179. (b) Lou, X. D.; Detrembleur, C.; Pagnouille, C.; Jerome, R.; Bocharova, V.; Kiriya, A.; Stamm, M. *Adv. Mater.* **2004**, *16*, 2123–2127.
- (11) Huang, H. M.; Liu, I. C.; Chang, C. Y.; Tsai, H. C.; Hsu, C. H.; Tsiang, R. C. C. *J. Polym. Sci., Part A: Polym. Chem.* **2004**, *42*, 5802–5810.
- (12) (a) Qin, S. H.; Qin, D. Q.; Ford, W. T.; Herrera, J. E.; Resasco, D. E. *Macromolecules* **2004**, *37*, 9963–9967. (b) Shaffer, M. S. P.; Koziol, K. *Chem. Commun.* **2002**, 2074–2075.
- (13) (a) Wang, J. W.; Khlobystov, A. N.; Wang, W. X.; Howdle, S. M.; Poliakov, M. *Chem. Commun.* **2006**, 1670–1672. (b) Dai, X. H.; Liu, Z. M.; Han, B. X.; Sun, Z. Y.; Wang, Y.; Xu, J.; Guo, X. L.; Zhao, N.; Chen, J. *Chem. Commun.* **2004**, 2190–2191.
- (14) Xu, H. X.; Wang, X. B.; Zhang, Y. F.; Liu, S. Y. *Chem. Mater.* **2006**, *18*, 2929–2934.
- (15) Petrov, P.; Lou, X. D.; Pagnouille, C.; Jerome, C.; Calberg, C.; Jerome, R. *Macromol. Rapid Commun.* **2004**, *25*, 987–990.
- (16) For example, see: (a) Zeng, H. L.; Gao, C.; Wang, Y. P.; Watts, P. C. P.; Kong, H.; Cui, X. W.; Yan, D. Y. *Polymer* **2006**, *47*, 113–122. (b) Gao, C.; Jin, Y. Z.; Kong, H.; Whitby, R. L. D.; Acquah, S. F. A.; Chen, G. Y.; Qian, H. H.; Hartschuh, A.; Silva, S. R. P.; Henley, S.; Fearon, P.; Kroto, H. W.; Walton, D. R. M. *J. Phys. Chem. B* **2005**, *109*, 11925–11932. (c) Nogales, A.; Broza, G.; Roslaniec, Z.; Schulte, K.; Sics, I.; Hsiao, B. S.; Sanz, A.; Garcia-Gutierrez, M. C.; Rueda, D. R.; Domingo, C.; Ezquerro, T. A. *Macromolecules* **2004**, *37*, 7669–7672.
- (17) (a) Xu, G. Y.; Wu, W. T.; Wang, Y. S.; Pang, W. M.; Wang, P. H.; Zhu, G. R.; Lu, F. *Nanotechnology* **2006**, *17*, 2458–2465. (b) You, Y. Z.; Hong, C. Y.; Pan, C. Y. *Nanotechnology* **2006**, *17*, 2350–2354. (c) Cui, H.; Wang, W. P.; You, Y. Z.; Liu, C. H.; Wang, P. H. *Polymer* **2004**, *45*, 8717–8721.
- (18) Hong, C. Y.; You, Y. Z.; Pan, C. Y. *Chem. Mater.* **2005**, *17*, 2247–2254.
- (19) Hong, C. Y.; You, Y. Z.; Pan, C. Y. *J. Polym. Sci., Part A: Polym. Chem.* **2006**, *44*, 2419–2427.
- (20) (a) Chen, S. M.; Chen, D. Y.; Wu, G. Z. *Macromol. Rapid Commun.* **2006**, *27*, 882–887. (b) Liu, I. C.; Huang, H. M.; Chang, C. Y.; Tsai, H. C.; Hsu, C. H.; Tsiang, R. C. C. *Macromolecules* **2004**, *37*, 283–287.
- (21) Zeng, H. L.; Gao, C.; Yan, D. Y. *Adv. Funct. Mater.* **2006**, *16*, 812–818.
- (22) (a) Qu, L. W.; Veca, L. M.; Lin, Y.; Kitaygorodskiy, A.; Chen, B. L.; McCall, A. M.; Connell, J. W.; Sun, Y. P. *Macromolecules* **2005**, *38*, 10328–10331. (b) Buffa, F.; Hu, H.; Resasco, D. E. *Macromolecules* **2005**, *38*, 8258–8263. (c) Gao, J. B.; Itkis, M. E.; Yu, A. P.; Bekyarova, E.; Zhao, B.; Haddon, R. C. *J. Am. Chem. Soc.* **2005**, *127*, 3847–3854.
- (23) Kong, H.; Gao, C.; Yan, D. *J. Am. Chem. Soc.* **2004**, *126*, 412–413.
- (24) Qin, S.; Qin, D.; Ford, W. T.; Resasco, D. E.; Herrera, J. E. *J. Am. Chem. Soc.* **2004**, *126*, 170–176.
- (25) Yao, Z.; Braidly, N.; Botton, G. A.; Adronov, A. *J. Am. Chem. Soc.* **2003**, *125*, 16015–16024.
- (26) Baskaran, D.; Mays, J. W.; Bratcher, M. S. *Angew. Chem., Int. Ed.* **2004**, *43*, 2138–2142.
- (27) Li, W. W.; Kong, H.; Gao, C.; Yan, D. Y. *Chin. Sci. Bull.* **2005**, *50*, 2276–2280.
- (28) Gao, C.; Vo, C. D.; Jin, Y. Z.; Li, W. W.; Armes, S. P. *Macromolecules* **2005**, *38*, 8634–8648.
- (29) (a) Kong, H.; Gao, C.; Yan, D. Y. *Macromolecules* **2004**, *37*, 4022–4030. (b) Qin, S. H.; Qin, D. Q.; Ford, W. T.; Resasco, D. E.; Herrera, J. E. *Macromolecules* **2004**, *37*, 752–757.
- (30) Kong, H.; Li, W. W.; Gao, C.; Yan, D. Y.; Jin, Y. Z.; Walton, D. R. M.; Kroto, H. W. *Macromolecules* **2004**, *37*, 6683–6686.
- (31) Sun, T.; Liu, H.; Song, W.; Wang, X.; Jiang, L.; Li, L.; Zhu, D. *Angew. Chem., Int. Ed.* **2004**, *43*, 4663–4666.
- (32) Kong, H.; Gao, C.; Yan, D. Y. *J. Mater. Chem.* **2004**, *14*, 1401–1405.
- (33) Qin, S. H.; Qin, D. Q.; Ford, W. T.; Herrera, J. E.; Resasco, D. E.; Bachilo, S. M.; Weisman, R. B. *Macromolecules* **2004**, *37*, 3965–3967.
- (34) Zhao, B.; Hu, H.; Haddon, H. C. *Adv. Funct. Mater.* **2004**, *14*, 71–76.
- (35) Lou, X. D.; Detrembleur, C.; Pagnouille, C.; Jerome, R.; Bocharova, V.; Kiriya, A.; Stamm, M. *Adv. Mater.* **2004**, *16*, 2123–2127.
- (36) (a) Riggs, J. E.; Guo, Z.; Carroll, D. L.; Sun, Y.-P. *J. Am. Chem. Soc.* **2000**, *122*, 5879–5880. (b) Riggs, J. E.; Walker, D. B.; Carroll, D. L.; Sun, Y.-P. *J. Phys. Chem. B* **2000**, *104*, 7071–7076.
- (37) Sano, M.; Kamino, A.; Shinkai, S. *Angew. Chem., Int. Ed.* **2001**, *40*, 4661–4663.
- (38) Chen, S. M.; Wu, G. Z.; Liu, Y. D.; Long, D. W. *Macromolecules* **2006**, *39*, 330–334.
- (39) Zhang, H.; Li, H. X.; Cheng, H. M. *J. Phys. Chem. B* **2006**, *110*, 9095–9099.
- (40) Li, W. W.; Gao, C.; Qian, H. F.; Ren, J. C.; Yan, D. Y. *J. Mater. Chem.* **2006**, *16*, 1852–1859.
- (41) Gao, C.; Li, W. W.; Morimoto, H.; Nagaoka, Y.; Maekawa, T. *J. Phys. Chem. B* **2006**, *110*, 7213–7220.
- (42) Gao, C.; Li, W. W.; Jin, Y. Z.; Kong, H. *Nanotechnology* **2006**, *17*, 2882–2890.
- (43) Hyperbranched polymers, for example, see: (a) Gao, C.; Yan, D. *Prog. Polym. Sci.* **2004**, *29*, 183–275. (b) Voit, B. *J. Polym. Sci., Part A: Polym. Chem.* **2005**, *43*, 2679–2699. (c) Jikei, M.; Kakimoto, M. *Prog. Polym. Sci.* **2001**, *26*, 1233–1285. (d) Kim, Y. H.; Webster, O. W. *Macromolecules* **1992**, *25*, 5561–5572. (e) Flory, P. J. *J. Am. Chem. Soc.* **1952**, *74*, 2718–2723.
- (44) Xu, Y. Y.; Gao, C.; Kong, H.; Yan, D. Y.; Jin, Y. Z.; Watts, P. C. P. *Macromolecules* **2004**, *37*, 8846–8853.
- (45) Cao, L.; Yang, W.; Yang, J.; Wang, C.; Fu, S. *Chem. Lett.* **2004**, *33*, 490–491.
- (46) Hong, C. Y.; You, Y. Z.; Wu, D. C.; Liu, Y.; Pan, C. Y. *Macromolecules* **2005**, *38*, 2606–2611.
- (47) Chen, G. X.; Kim, H. S.; Park, B. H.; Yoon, J. S. *J. Phys. Chem. B* **2005**, *109*, 22237–22243.
- (48) Yang, H.; Wang, S. C.; Mercier, P.; Akins, D. L. *Chem. Commun.* **2006**, 1425–1427.

- (49) (a) Gu, L. R.; Elkin, T.; Jiang, X. P.; Li, H. P.; Lin, Y.; Qu, L. W.; Tzeng, T. R. J.; Joseph, R.; Sun, Y.-P. *Chem. Commun.* **2005**, 874–876. (b) Gu, L. R.; Lin, Y.; Qu, L. W.; Sun, Y.-P. *Biomacromolecules* **2006**, *7*, 400–402.
- (50) (a) He, P.; Urban, M. W. *Biomacromolecules* **2005**, *6*, 2455–2457. (b) Zhang, Y. J.; Li, J.; Shen, Y. F.; Wang, M. J.; Li, J. H. *J. Phys. Chem. B* **2004**, *108*, 15343–15346. (c) Star, A.; Gabriel, J. C. P.; Bradley, K.; Gruner, G. *Nano Lett.* **2003**, *3*, 459–463. (d) Staii, C.; Johnson, A. T. *Nano Lett.* **2005**, *5*, 1774–1778. (e) Zheng, M.; Jagota, A.; Semke, E. D.; Diner, B. A.; Mclean, R. S.; Lustig, S. R.; Richardson, R. E.; Tassi, N. G. *Nat. Mater.* **2003**, *2*, 338–342. (f) Huang, X. Y.; McLean, R. S.; Zheng, M. *Anal. Chem.* **2005**, *77*, 6225–6228. (g) Singh, R.; Pantarotto, D.; McCarthy, D.; Chaloin, O.; Hoebeke, J.; Partidos, C. D.; Briand, J. P.; Prato, M.; Bianco, A.; Kostarelos, K. *J. Am. Chem. Soc.* **2005**, *127*, 4388–4396.
- (51) ATRP-relevant references, for example, see: (a) Pyun, J.; Kowalewski, T.; Matyjaszewski, K. *Macromol. Rapid Commun.* **2003**, *24*, 1043–1059. (b) Coessens, V.; Pintauer, T.; Matyjaszewski, K. *Prog. Polym. Sci.* **2001**, *26*, 337–377. (c) Pyun, J.; Matyjaszewski, K. *Chem. Mater.* **2001**, *13*, 3436–3448. (d) Matyjaszewski, K.; Xia, J. H. *Chem. Rev.* **2001**, *101*, 2921–2990. (e) Pyun, J.; Matyjaszewski, K. *Chem. Mater.* **2001**, *13*, 3436–3448. (f) Patten, T. E.; Xia, J. H.; Abernathy, T.; Matyjaszewski, K. *Science* **1996**, *272*, 866–868. (g) Wang, J. S.; Matyjaszewski, K. *J. Am. Chem. Soc.* **1995**, *117*, 5614–5615. (h) Kato, M.; Kamigaito, M.; Sawamoto, M.; Higashimura, T. *Macromolecules* **1995**, *28*, 1721–1723. (i) Kamigaito, M.; Ando, T.; Sawamoto, M. *Chem. Rev.* **2001**, *101*, 3689–3745.
- (52) Klein, J.; Herzog, D.; Hajibegli, A. *Makromol. Chem., Rapid Commun.* **1985**, *6*, 675–678.
- (53) (a) Mori, H.; Böker, A.; Krausch, G.; Müller, A. H. E. *Macromolecules* **2001**, *34*, 6871–6882. (b) Matyjaszewski, K.; Gaynor, S. G.; Kulfan, A.; Podwika, M. *Macromolecules* **1997**, *30*, 5192–5194.
- (54) Ohno, K.; Tsujii, Y.; Fukuda, T. *J. Polym. Sci., Part A: Polym. Chem.* **1998**, *36*, 2473–2481.
- (55) The biocompatibility of the glycopolymers has been investigated, see: Muthukrishnan, S.; Nitschke, M.; Gramm, S.; Özyürek, Z.; Voit, B.; Werner, C.; Müller, A. H. E. *Macromol. Biosci.* **2006**, *6*, 658–666.
- (56) (a) Muthukrishnan, S.; Zhang, M. F.; Burkhardt, M.; Drechsler, M.; Mori, H.; Müller, A. H. E. *Macromolecules* **2005**, *38*, 7926–7934. (b) Muthukrishnan, S.; Plamper, F.; Mori, H.; Müller, A. H. E. *Macromolecules* **2005**, *38*, 10631–10642.
- (57) (a) Liu, T. Q.; Jia, S. J.; Kowalewski, T.; Matyjaszewski, K.; Casado-Portilla, R.; Belmont, J. *Macromolecules* **2006**, *39*, 548–556. (b) Liu, T. Q.; Casado-Portilla, R.; Belmont, J.; Matyjaszewski, K. *J. Polym. Sci., Part A: Polym. Chem.* **2005**, *43*, 4695–4709. (c) Liu, T. Q.; Jia, S.; Kowalewski, T.; Matyjaszewski, K.; Casado-Portilla, R.; Belmont, J. *Langmuir* **2003**, *19*, 6342–6345. (d) Jin, Y. Z.; Gao, C.; Kroto, H. W.; Maekawa, T. *Macromol. Rapid Commun.* **2005**, *26*, 1133–1139.
- (58) For example, see: (a) Feng, W.; Brash, J.; Zhu, S. P. *J. Polym. Sci., Part A: Polym. Chem.* **2004**, *42*, 2931–2942. (b) Edmondson, S.; Huck, W. T. S. *J. Mater. Chem.* **2004**, *14*, 730–734. (c) Matyjaszewski, K.; Miller, P. J.; Shukla, N.; Immaraporn, B.; Gelman, A.; Luokkala, B. B.; Siclován, T. M.; Kickelbick, G.; Vallant, T.; Hoffmann, H.; Pakula, T. *Macromolecules* **1999**, *32*, 8716–8724. (d) Shah, R. R.; Merreceyes, D.; Husemann, M.; Rees, I.; Abbott, N. L.; Hawker, C. J.; Hedrick, J. L. *Macromolecules* **2000**, *33*, 597–605. (e) Edmondson, S.; Osborne, V. L.; Huck, W. T. S. *Chem. Soc. Rev.* **2004**, *33*, 14–22.
- (59) SCVP and SCVCP, for example, see: (a) Fréchet, J. M. J.; Henmi, M.; Gitsov, I.; Aoshima, S.; Leduc, M. R.; Grubbs, R. B. *Science* **1995**, *269*, 1080–1083. (b) Hawker, C. J.; Fréchet, J. M. J.; Grubbs, R. B.; Dao, J. *J. Am. Chem. Soc.* **1995**, *117*, 10763–10764. (c) Matyjaszewski, K.; Gaynor, S. G.; Müller, A. H. E. *Macromolecules* **1997**, *30*, 7034–7041. (d) Mori, H.; Seng, D. C.; Zhang, M. F.; Müller, A. H. E. *Langmuir* **2002**, *18*, 3682–3693. (e) Mori, H.; Seng, D. C.; Lechner, H.; Zhang, M. F.; Müller, A. H. E. *Macromolecules* **2002**, *35*, 9270–9281. (f) Mori, H.; Walther, A.; Andre, X.; Lanzendorfer, M. G.; Müller, A. H. E. *Macromolecules* **2004**, *37*, 2054–2066. (g) Cheng, C.; Wooley, K. L.; Khoshdel, E. *J. Polym. Sci., Part A: Polym. Chem.* **2005**, *43*, 4754–4770. (h) Hong, C. Y.; Pan, C. Y.; Huang, Y.; Xu, Z. D. *Polymer* **2001**, *42*, 6733–6740.
- (60) (a) Muthukrishnan, S.; Jutz, G.; André, X.; Mori, H.; Müller, A. H. E. *Macromolecules* **2005**, *38*, 9–18. (b) Muthukrishnan, S.; Mori, H.; Müller, A. H. E. *Macromolecules* **2005**, *38*, 3108–3119. (c) Muthukrishnan, S.; Erhard, D. P.; Mori, H.; Müller, A. H. E. *Macromolecules* **2006**, *39*, 2743–2750.
- (61) (a) Müller, A. H. E.; Yan, D. Y.; Wulkow, M. *Macromolecules* **1997**, *30*, 7015–7023. (b) Yan, D. Y.; Zhou, Z. P.; Müller, A. H. E. *Macromolecules* **1999**, *32*, 245–250.
- (62) Litvinenko, G. I.; Simon, P. F. W.; Müller, A. H. E. *Macromolecules* **1999**, *32*, 2410–2419.
- (63) Yan, D. Y.; Müller, A. H. E.; Matyjaszewski, K. *Macromolecules* **1997**, *30*, 7024–7033.
- (64) Matyjaszewski, K.; Pyun, J.; Gaynor, S. G. *Macromol. Rapid Commun.* **1998**, *19*, 665–670.

MA062238Z